

APPENDICES with Tables S1-S4 and Figures S1-S3

Appendix 1: Allometry

We estimated aboveground carbon density (ACD) in field plots using the general allometric approach outlined by Chave et al. [38], but with improvements to reflect regional allometric variation in Madagascar [39] (Table S1). In southern forests, we used regional models to estimate ACD as a function of stem diameter, height, and wood density. For the largest trees in each plot and a sampling of trees spanning a range of diameters, height was measured in the field. For all other trees, height was estimated as a function of stem diameter following Vieilledent et al. [39]. For northern forests, field plots were located above an altitude characterized by Vieilledent et al. [39], including regions of higher precipitation (e.g., wet or cloud forests). Here we estimated ACD using a global wet forest model of Chave et al. [38]. Again, we corrected for localized height variation by directly measuring the heights of the largest trees in all plots and additional trees spanning a range of stem diameter. For the remaining trees, we produced a model relating height and diameter using Maximum Likelihood Analysis in R (R Development Core Team, 2009); the fitting method follows that described in the methods section of the LiDAR MCH-to-ACD model. For all trees across the study region, wood density values were assigned based on plant genera-level field identification using a combination of regional field-based estimates Vieilledent et al. [39] and values from a global wood density database (Table S2). For those species without a field or literature estimate, a default value of the regional mean wood density was used.

Appendix 2: Spatial resolution of LiDAR calibration

Airborne LiDAR mapping errors are a function of the regression error (RMSE) for a given calibration model, which itself is dependent on the spatial resolution (or plot size) used to construct the calibration [38]. In this case, the largest plots were 30m in radius (0.2827 ha), and thus our calibration error (21.1 Mg C ha⁻¹) conservatively applies to a LiDAR-derived carbon maps with a spatial resolution of 0.2827 ha. With an iterative analysis across several spatial resolutions, Mascaro et al. [14] showed that, for spatial resolutions up to 1 ha, prediction errors decline in accordance with the general influence of sample size on the standard error of the mean. That is, errors decline as a function of the inverse square root of the plot size or spatial resolution. Following this, our predicted LiDAR-based error is 11.2 Mg C ha⁻¹ at 1 ha spatial resolution.

Appendix 3: LiDAR-scale statistics within vegetation classes

Complete LiDAR-scale results for the northern region are given in Table S3, and results for the southern region are given in Table S4. Forest regrowth classes in the southern spiny forest region (e.g., below 500 m) are likely overestimated due to uncertainty caused by phenology. However, these classifications still translate into improved fidelity in the final carbon maps because these regrowth classes are associated with a much lower ACD values as directly measured by airborne LiDAR.

Appendix 4: Controls over LiDAR-derived ACD variation

Following the results of the correlation analyses (see Methods of main text), we conducted multiple linear regression analyses using elevation derived from NASA Shuttle Radar Topography Mission (SRTM) data (DEM) and photosynthetic vegetation coverage fraction (PV) derived from CLASlite. In the northern region, this analysis yielded the following model:

$$\text{ACD} = 0.3139 \text{ DEM} - 0.0001 \text{ DEM}^2 + 3.1800 \text{ PV} - 404.5$$

with an adjusted r^2 of 0.27 ($P < 0.0001$) and a standard error of $41.8 \text{ Mg C ha}^{-1}$. In the southern region, the analysis yielded the following model:

$$\text{ACD} = 0.2121 \text{ DEM} - 0.0001 \text{ DEM}^2 + 2.0746 \text{ PV} - 165.3$$

with an adjusted r^2 of 0.67 ($P < 0.0001$) and a standard error of $31.5 \text{ Mg C ha}^{-1}$.

Table S1. Allometric equations used to estimate height (H) in meters (m) and aboveground biomass (AGB in kg) based on stem diameter at 1.3 m aboveground (dbh) or above buttress (D in cm), and wood specific gravity (ρ in g cm⁻³).

Region	Par.	Equation	r^2	Reference
N Humid	AGB	$0.0776 \cdot (D^2 \cdot H \cdot \rho)^{0.94}$	0.96*	Chave et al. 2005 [38]
N Humid	H	$2.4661 \cdot D^{0.5659}$	0.70	This study
S Humid	AGB	$\exp(-1.948 + 1.969 \cdot \ln(D) + 0.66 \cdot \ln(H) + 0.828 \cdot \ln(\rho))$	0.90*	Vieilledent et al. [39]
S Humid	H	$\exp(1.103 + 0.529 \cdot \ln(D))$	0.95*	Vieilledent et al. [39]
S Dry	AGB	$\exp(-1.103 + 1.994 \cdot \ln(D) + 0.317 \cdot \ln(H) + 1.303 \cdot \ln(\rho))$	0.95*	Vieilledent et al. [39]
S Dry	H	$12.12 - (12.12 - 1.3) \cdot \exp(-0.52 \cdot D)$	0.89*	Vieilledent et al. [39]

*coefficient of determination for $\ln(y)$

Table S2. Wood density values used to estimate aboveground biomass in field plots. Values are based on either samples by Vieilledent et al. [39] or a global wood density database by Chave et al. [31]. For those species with neither field nor literature estimates, we used a default value of the regional mean wood density.

Genus	Wood Density (g cm ⁻³)		Number of Stems			Reference
	Humid	Spiny	Northern		Southern	
			n	Humid	Humid	
<i>Asteropeia</i>	0.79		1	0	0	Chave
<i>Adina</i>	0.59		0	3	0	Chave
<i>Albizia</i>	0.66	0.56	5	25	42	Vieilledent
<i>Alluaudia</i>		0.31	0	0	808	Vieilledent
<i>Anthocleista</i>	0.79		0	3	0	Vieilledent
<i>Aspidostemon</i>	0.71		7	0	0	Chave
<i>Bathiorhamnus</i>	0.57		2	0	0	Chave
<i>Bembicia</i>	0.69		10	0	0	Chave
<i>Breonia</i>	0.73		0	27	0	Chave
<i>Brochoneura</i>	0.50		0	9	0	Vieilledent
<i>Calophyllum</i>	0.67		2	1	0	Vieilledent
<i>Canarium</i>	0.47		12	17	0	Vieilledent
<i>Canthium</i>	0.84		2	0	0	Chave
<i>Capurodendron</i>		0.80	0	0	3	Chave
<i>Cedrelopsis</i>		0.74	0	0	49	Vieilledent
<i>Chrysophyllum</i>	0.53		0	65	0	Vieilledent
<i>Commiphora</i>		0.24	0	0	976	Vieilledent
<i>Croton</i>	0.55	0.85	14	1	9	Vieilledent
<i>Cryptocarya</i>	0.53		50	0	0	Vieilledent
<i>Cynometra</i>	0.77		0	3	0	Chave
<i>Dalbergia</i>	0.74	0.74	0	8	3	Chave
<i>Dichrostachys</i>		0.79	0	0	4	Chave
<i>Dilobeia</i>	0.79		0	2	0	Chave
<i>Diospyros</i>	0.79	0.77	5	19	6	Vieilledent
<i>Dombeya</i>	0.27		52	16	0	Vieilledent
<i>Ehretia</i>	0.51		1	0	0	Chave
<i>Elaeocarpus</i>	0.50		16	48	0	Chave
<i>Erythroxylum</i>	0.68		30	0	0	Vieilledent
<i>Eugenia</i>	0.64		0	10	0	Vieilledent
<i>Euphorbia</i>		0.39	0	0	684	Vieilledent
<i>Ficus</i>	0.49		14	4	0	Vieilledent
<i>Garcinia</i>	0.69		1	0	0	Chave
<i>Givotia</i>	0.19		2	0	0	Chave
<i>Grewia</i>	0.36	0.69	0	13	9	Vieilledent
<i>Gyrocarpus</i>		0.31	0	0	98	Vieilledent
<i>Harungana</i>	0.47		61	50	0	Vieilledent

<i>Homalium</i>	0.77		24	19	0	Vieilledent
<i>Hymenodictyon</i>		0.48	0	0	32	Chave
<i>Hyperacanthus</i>	0.69		0	6	0	Chave
<i>Intsia</i>	0.69		1	0	0	Chave
<i>Khaya</i>	0.53		0	5	0	Chave
<i>Macarisia</i>	0.62		0	7	0	Chave
<i>Magnistipula</i>	0.81		0	4	0	Chave
<i>Mammea</i>	0.71		0	11	0	Chave
<i>Mascarenhasia</i>	0.64		2	0	0	Chave
<i>Neobeguea</i>		0.84	0	0	7	Chave
<i>Noronhia</i>	0.78		4	0	0	Vieilledent
<i>Ocotea</i>	0.57		20	49	0	Vieilledent
<i>Oncostemum</i>	0.51		5	0	0	Chave
<i>Operculicarya</i>		0.22	0	0	249	Vieilledent
<i>Pachypodium</i>		0.10	0	0	48	Vieilledent
<i>Phyllarthron</i>	0.89		1	0	0	Chave
<i>Pittosporum</i>	0.51		1	0	0	Chave
<i>Polyalthia</i>	0.53		0	1	0	Chave
<i>Polyscias</i>	0.48		0	1	0	Chave
<i>Poupartia</i>	0.36		0	7	0	Chave
<i>Protorhus</i>	0.65		5	1	0	Chave
<i>Prunus</i>	0.66		2	0	0	Chave
<i>Rhus</i>		0.62	0	0	1	Vieilledent
<i>Scolopia</i>	0.75		0	18	0	Chave
<i>Securinega</i>		0.80	0	0	34	Vieilledent
<i>Sideroxylon</i>	0.80		0	1	0	Chave
<i>Stereospermum</i>		0.77	0	0	16	Chave
<i>Streblus</i>	0.63		1	12	0	Vieilledent
<i>Strychnos</i>		0.73	0	0	8	Vieilledent
<i>Sympmania</i>	0.64		0	12	0	Vieilledent
<i>Syzygium</i>	0.68		60	1	0	Vieilledent
<i>Tamarindus</i>		0.87	0	0	2	Chave
<i>Tambourissa</i>	0.51		34	43	0	Vieilledent
<i>Terminalia</i>	0.62	0.71	1	0	21	Vieilledent
<i>Tetrapterocarpon</i>		0.73	0	0	4	Vieilledent
<i>Trema</i>	0.37		9	1	0	Chave
<i>Uapaca</i>	0.60		0	7	0	Vieilledent
<i>Vepris</i>	0.56		0	13	0	Chave
<i>Vitex</i>	0.60		0	1	0	Chave
<i>Weinmannia</i>	0.62		24	14	0	Vieilledent
<i>Xylopia</i>	0.51		7	8	0	Chave
<i>Zanthoxylum</i>	0.51	0.51	1	0	4	Chave
Others	0.61	0.35	432	253	175	(mean)
Total			921	819	3292	

Table S3. LiDAR statistics for the northern region. ACD is aboveground carbon density (Mg C ha⁻¹).

PV Fraction	DEM (m)	ACD Mean	ACD Median	ACD Standard Deviation	LiDAR Coverage (ha)
<i>Forest</i>					
80 - 90	Below 751	28.7	23.4	21.6	57.0
80 - 90	751 - 900	35.2	23.5	36.0	190.9
80 - 90	901 - 1050	48.1	35.9	48.0	243.9
80 - 90	1051 - 1200	75.8	72.7	60.3	489.2
80 - 90	1201 - 1350	71.9	62.8	62.8	1011.9
80 - 90	1351 - 1500	81.9	73.4	63.3	2317.8
80 - 90	1501 - 1650	104.8	109.0	53.5	2889.7
80 - 90	1651 - 1800	95.8	100.5	48.2	3894.2
80 - 90	1801 - 1950	75.3	73.5	40.8	4127.5
80 - 90	1951 - 2100	55.7	50.8	33.4	2958.1
80 - 90	2101 - 2250	40.0	38.6	24.8	1411.9
80 - 90	2251 - 2400	33.0	33.0	18.9	572.7
80 - 90	Above 2400	22.0	20.3	17.1	19.7
91 - 100	Below 751	44.1	37.5	32.5	57.6
91 - 100	751 - 900	58.2	54.7	40.2	198.6
91 - 100	901 - 1050	94.0	89.9	57.4	416.4
91 - 100	1051 - 1200	117.2	111.3	63.8	1261.5
91 - 100	1201 - 1350	118.5	113.2	63.7	1832.5
91 - 100	1351 - 1500	119.8	121.3	60.1	2743.4
91 - 100	1501 - 1650	118.9	123.1	55.8	3237.4
91 - 100	1651 - 1800	105.5	110.6	49.1	3239.0
91 - 100	1801 - 1950	86.1	85.7	41.5	2518.7
91 - 100	1951 - 2100	70.4	66.2	34.5	847.7
91 - 100	2101 - 2250	55.5	55.6	25.9	343.8
91 - 100	2251 - 2400	35.9	36.0	19.9	200.7
91 - 100	Above 2400	14.4	14.8	13.3	7.1
<i>Non-Forest</i>					
0 - 20	Full Range	3.2	0.5	8.2	353.0
21 - 40	Full Range	3.9	0.3	10.8	1141.7
41 - 60	Full Range	7.9	1.1	17.7	2195.3
61 - 80	Full Range	19.4	4.7	31.7	6257.4
81 - 100	Full Range	43.3	31.8	43.1	328.5
<i>Deforestation Regrowth - 5 Years</i>					
80 - 100	Full Range	39.4	33.4	29.4	84.0
<i>Deforestation Regrowth - 10 Years</i>					
80 - 100	Full Range	52.9	40.2	49.5	125.3
<i>Disturbance Regrowth - All</i>					
80 - 100	Full Range	70.9	54.5	56.6	42.5

Table S4. LiDAR statistics for the southern region. ACD is aboveground carbon density (Mg C ha⁻¹).

PV Fraction	DEM (m)	ACD Mean	ACD Median	ACD Standard Deviation	LiDAR Coverage (ha)
<i>Forest</i>					
60 - 69	1 - 100	11.7	11.1	7.1	1160.2
60 - 69	101 - 200	12.9	12.8	8.2	2037.2
60 - 69	201 - 300	10.8	9.8	8.9	639.8
60 - 69	301 - 400	12.3	10.6	12.3	562.1
60 - 69	401 - 500	13.7	7.7	21.5	137.8
60 - 69	501 - 700	18.3	8.2	28.0	120.0
60 - 69	701 - 900	21.7	11.8	29.0	47.0
60 - 69	901 - 1100	15.1	3.0	28.5	49.1
60 - 69	1101 - 1300	29.0	8.2	38.6	26.3
60 - 69	1301 - 1500	29.8	15.9	30.8	15.8
60 - 69	1501 +	34.8	30.2	28.6	4.0
70 - 79	1 - 100	14.2	14.1	5.9	2454.3
70 - 79	101 - 200	17.1	17.1	7.7	3949.0
70 - 79	201 - 300	14.3	13.1	12.4	742.4
70 - 79	301 - 400	17.4	14.3	21.0	593.8
70 - 79	401 - 500	24.2	13.5	35.2	269.7
70 - 79	501 - 700	36.5	18.5	44.7	202.3
70 - 79	701 - 900	43.5	24.1	45.2	128.4
70 - 79	901 - 1100	45.9	30.4	45.2	114.8
70 - 79	1101 - 1300	59.5	59.2	41.7	93.4
70 - 79	1301 - 1500	49.6	51.8	33.0	75.5
70 - 79	1501 +	44.7	39.9	30.2	30.8
80 - 89	1 - 100	18.6	18.1	7.4	1304.4
80 - 89	101 - 200	19.5	19.3	7.2	4004.2
80 - 89	201 - 300	20.5	18.3	19.2	1135.5
80 - 89	301 - 400	38.9	17.3	51.7	596.3
80 - 89	401 - 500	74.1	38.7	70.2	586.1
80 - 89	501 - 700	122.3	131.6	66.9	1076.0
80 - 89	701 - 900	111.3	115.6	50.9	1055.5
80 - 89	901 - 1100	94.4	95.9	37.8	1080.4
80 - 89	1101 - 1300	80.9	81.1	32.0	842.9
80 - 89	1301 - 1500	69.9	70.3	27.4	529.4
80 - 89	1501 +	59.6	59.4	26.4	121.3
90 - 100	1 - 100	32.6	27.0	24.5	79.7
90 - 100	101 - 200	24.1	21.9	14.6	398.6
90 - 100	201 - 300	31.6	22.1	31.8	898.8
90 - 100	301 - 400	61.3	27.9	58.0	794.6
90 - 100	401 - 500	104.1	115.5	69.2	894.3
90 - 100	501 - 700	146.5	152.2	57.0	2618.4
90 - 100	701 - 900	135.5	137.1	47.9	3175.8
90 - 100	901 - 1100	109.9	110.1	38.6	2692.7
90 - 100	1101 - 1300	89.8	89.4	32.7	1994.4
90 - 100	1301 - 1500	80.4	79.7	30.7	1022.2
90 - 100	1501 +	75.1	77.0	29.2	437.2

Non-Forest

0 - 20	0 - 500	2.8	0.9	4.8	6264.5
21 - 40	0 - 500	5.4	3.2	6.9	5723.0
41 - 60	0 - 500	8.6	6.9	8.9	8190.5
61 - 80	0 - 500	13.5	6.3	22.3	470.3
81 - 100	0 - 500	22.7	9.7	33.1	1149.8
0 - 20	Above 500	1.7	0.0	6.1	164.6
21 - 40	Above 500	5.8	1.3	12.5	200.7
41 - 60	Above 500	14.1	4.1	25.6	399.6
61 - 80	Above 500	48.9	31.7	47.7	197.4
81 - 100	Above 500	67.6	59.1	53.6	754.1

Deforestation Regrowth - 5 Years

80 - 100	0 - 500	18.8	18.4	8.5	3310.6
80 - 100	Above 500	33.9	19.2	42.8	78.9

Deforestation Regrowth - 10 Years

80 - 100	0 - 500	16.1	16.1	8.1	1474.1
80 - 100	Above 500	21.6	18.4	22.1	27.5

Disturbance Regrowth - All

80 - 100	0 - 500	18.1	17.6	8.1	843.2
80 - 100	Above 500	49.2	30.0	50.1	30.3

Appendix Figures

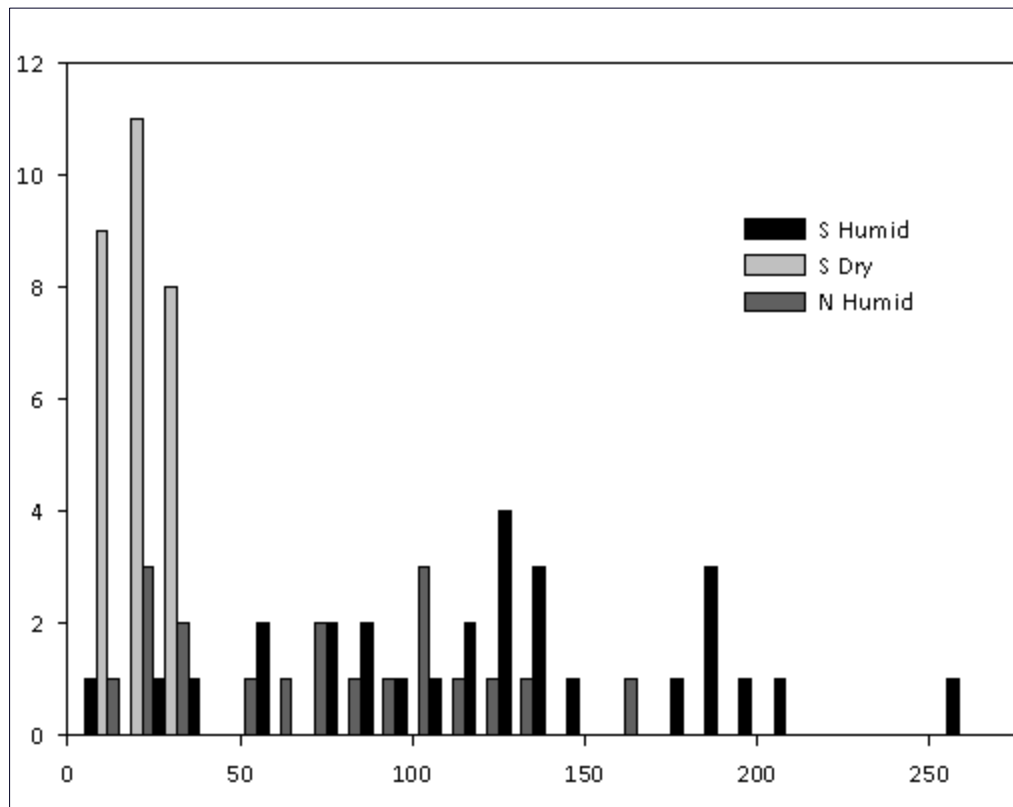


Figure S1. Variation in plot-level aboveground carbon density (ACD) according to general forest type in Madagascar.

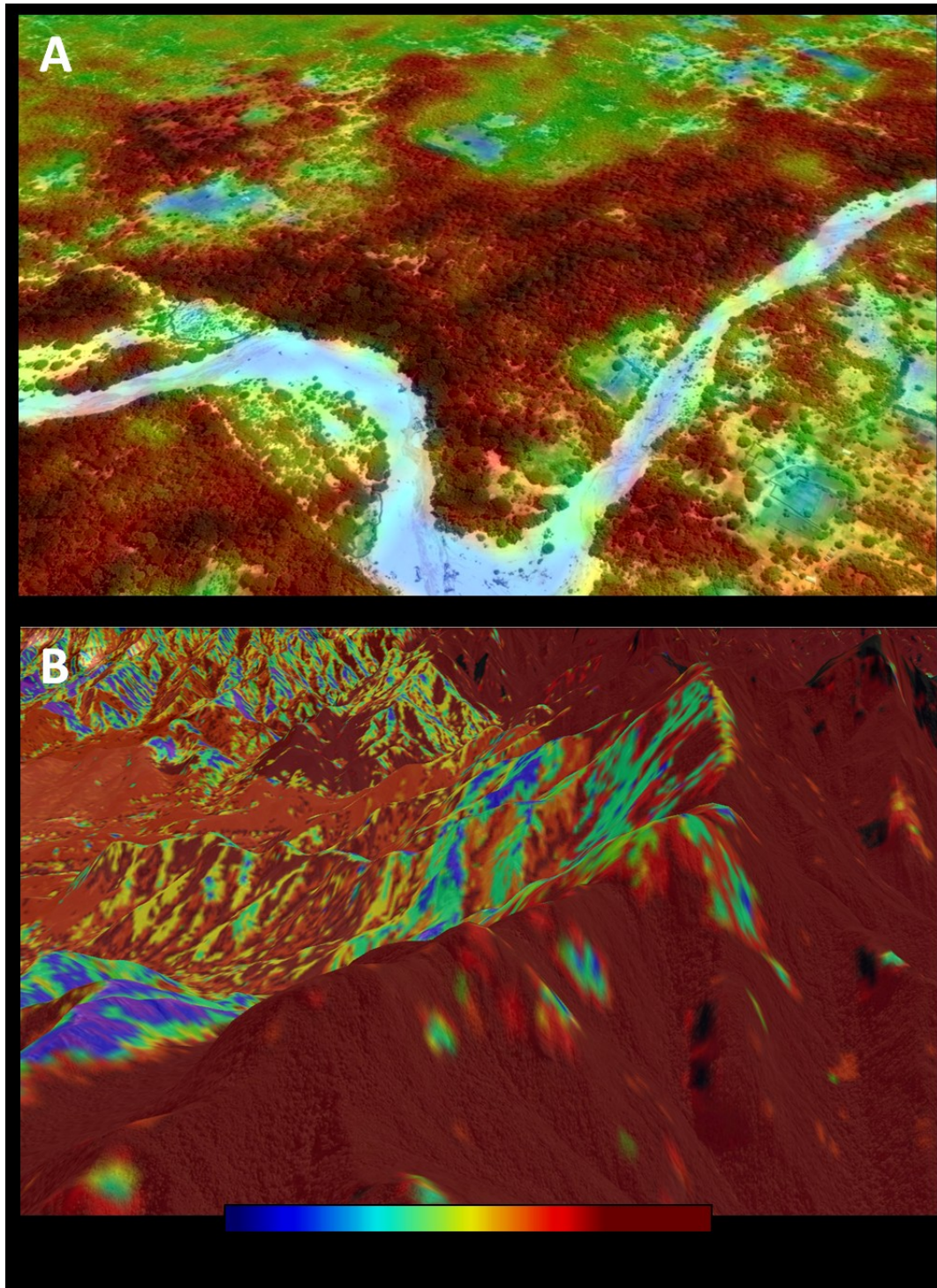


Figure S2. Comparisons of regionally extrapolated aboveground carbon density (ACD) overlaid on high-resolution vegetation imagery from Google Earth. Notice how the regional mapping estimates of high (red) to low (blue) carbon stocks align spatially with the observed distribution of trees in the Google Earth imagery.

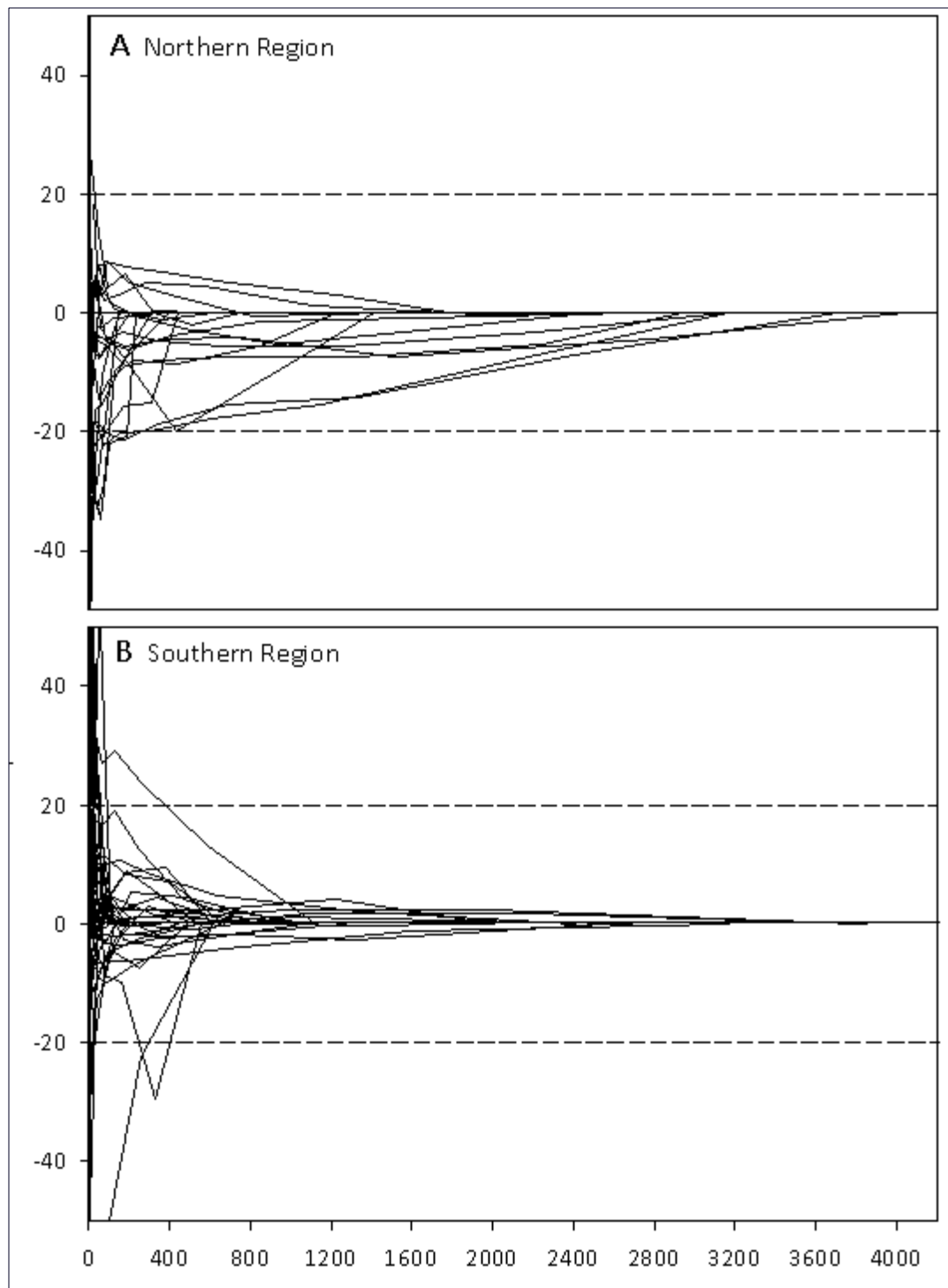


Figure S3. Change in normalized median carbon density (on a percentage basis) derived from airborne LiDAR relative to the total LiDAR coverage for 26 vegetation classes in the N region and 44 in the S region. Thus the median carbon density for successive LiDAR extents was compared based on the percentage by which they differed from the median value at full coverage.